Eur Biophys J (2010) 39:1407–1419
DOI 10.1007/s00249-010-0595-x

ORIGINAL PAPER

The structure of dopamine induced α-synuclein oligomers

Agata Rekas · Robert B. Knott · Anna Sokolova · Kevin J. Barnham · Keyla A. Perez · Colin L. Masters · Simon C. Drew · Roberto Cappai · Cyril C. Curtain · Chi L. L. Pham

Received: 9 October 2009 / Revised: 22 February 2010 / Accepted: 28 February 2010 / Published online: 23 March 2010

Abstract Inclusions of aggregated α-synuclein (α-syn) in dopaminergic neurons are a characteristic histological marker of Parkinson's disease (PD). In vitro, α-syn in the presence of dopamine (DA) at physiological pH forms SDS-resistant non-amyloidogenic oligomers. We used a combination of biophysical techniques, including sedimentation velocity analysis, small angle X-ray scattering (SAXS) and circular dichroism spectroscopy to study the characteristics of α-syn oligomers formed in the presence of DA. Our SAXS data show that the trimers formed by the action of DA on α-syn consist of overlapping worm-like monomers, with no end-to-end associations. This lack of structure contrasts with the well-established, extensive β-sheet structure of the amyloid fibril form of the protein and its pre-fibrillar oligomers. We propose on the basis of these and earlier data that oxidation of the four methionine residues at the C- and N-terminal ends of α-syn molecules prevents their end-to-end association and stabilises oligomers formed by cross linking with DA-quinone/DA-melanin, which are formed as a result of the redox process, thus inhibiting formation of the β-sheet structure found in other pre-fibrillar forms of α-syn.

Keywords Parkinson's disease · α-Synuclein · Dopamine · Protein aggregation · SAXS · CD spectroscopy · EPR spectroscopy · Sedimentation velocity analysis

Abbreviations

Aβ	The β-peptide of AD amyloid
AD	Alzheimer's disease
α-syn	α-Synuclein
α-syn:DA	α-Synuclein:dopamine
CD	Circular dichroism
DA	Dopamine
EDTA	Ethylenediamine tetraacetic acid
EPR	Electron paramagnetic resonance spectroscopy
HMW	High molecular weight
PAGE	Polyacrylamide gel electrophoresis
PD	Parkinson's disease
SAXS	Small-angle X-ray scattering
SDS	Sodium dodecyl sulphate
SEC	Size-exclusion chromatography
SVA	Sedimentation velocity analysis

A. Rekas · R. B. Knott · A. Sokolova
Australian Nuclear Science and Technology Organisation (ANSTO), Menai, NSW, Australia

K. J. Barnham · K. A. Perez · S. C. Drew · R. Cappai · C. C. Curtain · C. L. L. Pham
Department of Pathology, The University of Melbourne, Melbourne, VIC 3010, Australia

K. J. Barnham · K. A. Perez · S. C. Drew · R. Cappai · C. C. Curtain · C. L. L. Pham
Bio21 Molecular Science and Technology Institute, The University of Melbourne, Melbourne, VIC 3010, Australia

K. J. Barnham · K. A. Perez · C. L. Masters · S. C. Drew · C. C. Curtain · C. L. L. Pham
Mental Health Research Institute, Parkville, VIC 3052, Australia

S. C. Drew · C. C. Curtain
School of Physics, Monash University, Clayton, VIC 3080, Australia

A. Rekas (✉)
ANSTO, Locked Bag 2001, Kirrawee DC, NSW 2232, Australia
e-mail: agata.rekas@ansto.gov.au

Introduction

α-Synuclein (α-syn), a 140 residue natively unfolded protein, is implicated in a spectrum of neurodegenerative diseases, including common conditions such as Parkinson's disease (PD), which affects 1–2% of people world-wide, and the less common dementia with Lewy bodies, and the Lewy body variant of Alzheimer's disease (AD). The α-syn gene (PARK 1) was the first to be linked with PD when two mis-sense mutations (A30P and A53T) were identified in familial PD (El-Agnaf et al. 1998; Polymeropoulos et al. 1997). PD is characterised by the selective degeneration of dopaminergic neurons and the presence of insoluble α-syn aggregates, i.e. amyloid fibrils, deposited in Lewy bodies in the remaining substantia nigra neurons of the mid-brain. This region of the brain plays an important role in reward, addiction and the control of movement and balance, processes mediated by dopamine (DA) in its neurotransmitter role.

The dopaminergic neuron loss and the alleviation of clinical symptoms for a period by administering L-dopa suggest that there is a link between α-syn aggregation and DA metabolism. Conway et al. (2001) found that DA-quinone, produced by the Fe-based oxidation of DA, kinetically stabilised α-syn protofibrils, and they proposed that the formation of 'DA-α-syn adducts' (DA-modified α-syn) provided an explanation for the dopaminergic pathway of α-syn-associated neurotoxicity in PD. L-dopa, DA and other catecholamines disaggregate in vitro generated fibrils (Li et al. 2004) and also inhibit fibrillisation of α-syn (Li et al. 2004; Norris et al. 2005; Conway et al. 2001). Furthermore, in the presence of DA, α-syn forms soluble, SDS-resistant oligomers that are not amyloidogenic and lack the typical amyloid fibril structures since they do not bind thioflavin T (Cappai et al. 2005). These findings suggest that DA is a dominant modulator of α-syn aggregation. DA readily undergoes oxidation to generate reactive quinone intermediates and several studies have suggested the roles of DA oxidative intermediates in promoting α-syn oligomerisation and fibril disaggreation (Norris et al. 2005; Li et al. 2004; Pham et al. 2009; Burke et al. 2008). Dopaminochrome, an oxidation product of DA, reversibly inhibited α-syn fibrillisation by forming small soluble oligomers (Norris et al. 2005; Li et al. 2004). More recently, it was shown that the reactive DA oxidation intermediate 5,6-dihydroxylindole is involved in the formation of soluble α-syn oligomers at the physiological pH (7.4), although at pH 4.0 it promotes the formation of SDS-resistant insoluble oligomers that further associate to form sheet-like assemblies of fibrils (Pham et al. 2009). Another pointer to this role for DA oxidation intermediates is the finding by Burke et al. (2008) that the monoamine oxidase metabolite of DA, 3,4-dihydroxyphenylacetaldehyde (DOPAL), triggered α-syn aggregation in a cell-free system and in neuronal cell cultures resulting in the formation of potentially toxic α-syn oligomers and aggregates. They also showed that DOPAL injection into the substantia nigra of Sprague-Dawley rats resulted in dopaminergic neuron loss and the accumulation of high molecular weight (HMW) oligomers of α-syn. These results suggested that distinct reactive intermediates of DA, and not DA itself, interacted with α-syn and induced its oligomerisation.

However, the details of interaction between α-syn and DA (or its oxidative intermediates) are yet to be elucidated. Conway et al. (2001) suggested that the DA-modification of α-syn stabilised the oligomers and prevented them from elongating into mature fibrils. In agreement with this mode of mechanism, Li et al. (2004) have suggested that the covalent modification of α-syn molecules by DA reactive quinone leads to the formation of stable oligomers and weakening of the intermolecular forces of the α-syn fibrils, resulting in the disaggregation of fibrils into soluble oligomers and monomers (Li et al. 2004). By contrast, it has been argued that the inhibition of α-syn fibrillisation by DA and its oxidative intermediates does not involve any covalent modification of α-syn because mutagenesis of key amino acids (Met, His and Tyr) that might undergo modification did not abrogate this inhibition (Norris et al. 2005). Instead, DA oxidative intermediates may have interacted with α-syn residues 125–129 (the "YEMPS" sequence), induced structural changes in α-syn and promoted the formation of off-pathway oligomers (Norris et al. 2005). However, a recent study demonstrated that the formation of the DA-mediated α-syn oligomers did not require the YEMPS sequence because a truncated α-syn mutant terminating at residue 124 could still form soluble oligomers in the presence of DA (Leong et al. 2009a, b). The observations that DA-mediated α-syn oligomerisation was accompanied by the oxidation of all four Met residues within α-syn (Norris et al. 2005; Leong et al. 2009a, b) and mutagenesis of all four Met residues to Ala significantly reduced the propensity of α-syn to form SDS-resistant soluble oligomers suggesting that Met oxidation of α-syn might be the key mechanism by which DA mediated the formation of α-syn soluble oligomers and prevented the conversion of soluble oligomers into amyloid fibrils (Leong et al. 2009a, b).

Electron microscopy (Cappai et al. 2005) showed that α-syn incubated with DA gave rise to species with a variety of sizes and shapes, but provided no information about their supra-molecular structure and, therefore, mode of association. Such information may be important in elucidating the role of DA and oligomeric α-syn in PD. Application of conventional structure-determining techniques, such as X-ray crystallography and NMR is limited because of the

size and nature of the oligomers. However, recent advances in molecular shape modelling from small angle X-ray scattering (SAXS) data, e.g. the DAMMIN / DAMMIF program (Svergun 1997; Konarev et al. 2006) make it possible to accomplish low-resolution shape and internal structure retrieval ab initio, not requiring a foreknowledge of the high-resolution structure of the subunits of supramolecular assemblages. In this paper, we report the use of SAXS measurements, combined with circular dichroism (CD) spectroscopy and sedimentation velocity analysis (SVA), to describe the morphology of the trimers formed at the beginning of the oligomerisation of α-syn in the presence of DA and to relate this morphology to current knowledge of the formation of DA-induced α-syn oligomers.

Experimental

Expression of recombinant α-syn

α-Syn was overexpressed in *Escherichia coli* BL21 (DE3) cell strain transformed with pRSETB expression plasmid containing α-syn DNA sequence. The purification of α-syn was performed as described previously (Cappai et al. 2005). Briefly, the expression cell pellets were resuspended in lysis buffer [20 mM Tris-HCl pH 7.5, 5 mM EDTA and protease inhibitor EDTA-free tablet (Roche)]. The cells were lysed by sonication and centrifuged at 16,000 rpm for 1 h at 4°C using an Avanti centrifuge (Beckman). The pellet was discarded and soluble lysate was subjected to acid precipitation followed by anion exchange chromatography using a 5 mL HiTrap Q® HP column (GE Healthcare) equilibrated with 10 mM Tris-HCl, pH 7.5. The protein was eluted from the column using 0–1.0 M NaCl gradient. The pooled fractions containing α-syn were dialysed against MilliQ® water and lyophilised. The lyophilised protein was dissolved in 100 mM ammonium bicarbonate pH 7.5 and loaded onto a size exclusion chromatography (SEC) HiPrep Sephacryl® S300 26/60 column (GE Healthcare) equilibrated in 100 mM ammonium bicarbonate pH 7.5. The eluted protein was pooled and dialysed against MilliQ® water before being lyophilised. The purity of the protein was determined by SDS-PAGE analysis and mass spectrometry. The protein concentration was determined using the 280 nm extinction coefficient of 5,120 M^{-1} cm^{-1}.

Preparation of DA-treated α-syn samples

The lyophilised α-syn was dissolved in 6 M guanidine hydrochloride, 10 mM Tris-HCl at pH 7.5 to a concentration of approximately 450 μM. Buffer exchange was performed on a PD-10 desalting column (GE Healthcare) equilibrated in MilliQ® water. The eluted protein was filtered through a 0.22 μm syringe-driven filter and then diluted into buffer containing DA. The final composition of the sample was 200 μM of α-syn and 2 mM DA in 10 mM sodium phosphate at pH 7.4. About 10–20 mL of this sample was incubated at 37°C for 5–7 days. Samples were subjected to high-speed centrifugation in a TL-100 ultracentrifuge (Beckman, USA) at 390,880 *g* (100,000 rpm) for 45 min at 4°C, and the supernatants (soluble oligomer fractions) were collected for SEC using a HiLoad Superdex 200 16/60 column (GE Healthcare). For each run, 2 mL of soluble fraction was loaded onto the column equilibrated with 10 mM sodium phosphate at pH 7.4. Oligomers were eluted from the column at a flow rate of 1 mL/min and 1 mL fractions were collected. Multiple runs of SEC for α-syn:DA oligomers were performed and the elution profiles for all the runs were consistent. Accordingly, the eluted fractions from multiple SEC runs were combined and a 15 μL sample of each fraction was used for SDS-PAGE/silver stain analysis using 12% Bis-Tris gel (Invitrogen).

For SAXS and parallel CD measurements, the eluted fractions were lyophilised and re-dissolved in MilliQ® water immediately before use. For sedimentation velocity analysis, CD and EPR measurements, the eluted fractions were concentrated three- to eight-fold using ultrafiltration centrifugation (Millipore).

Sedimentation velocity analysis (SVA)

The concentrated fractions from SEC were diluted with 10 mM sodium phosphate at pH 7.4 so that the $OD_{280\ nm}$ of each sample was between 0.5–1.0. Samples (380 μL) and reference (400 μL) solutions were loaded into a double sector quartz cell fitted with a 12 mm thick centrepiece and placed in a Beckman An-60 Ti rotor. HMW oligomer samples were centrifuged at 25,000 rpm while the dimer and trimer fractions were centrifuged at 35,000 rpm and the monomer samples were centrifuged at 40,000 rpm for 16 h at 20°C in a Beckman XL-I analytical ultracentrifuge (Beckman Coulter, CA). Radial absorbance data were collected at a wavelength of 280 nm every 9.5 min with radial increments of 0.002 cm in a continuous scanning mode. For each sample, the sedimentation velocity profiles were fitted to the c(M) models with the aid of the freeware computer program SEDFIT (http://www.analyticalultracentrifugation.com/sizedistributions.htm) using a regularisation parameter of $P = 0.95$ with a resolution of 100. Time-independent and radial-independent noise was fitted. The sample meniscus position and the frictional ratio (f/f_0) were routinely fitted. The smallest molar mass (M-min) was set at 0.35 kDa and the largest molar mass (M-max) was set at 1,500 kDa for HMW oligomeric samples and 300 kDa for the LMW oligomeric samples.

MALDI TOF mass spectrometry

Samples (5 μL) of SEC fractions 31, 20 and 16, corresponding to Met-oxidised α-syn monomer, α-syn:DA dimer and α-syn:DA trimer, were spotted onto a H50 Protein Chip array (Bio-Rad) and allowed to air-dry. Each spot was washed with 10 μl of 100 mM HEPES and allowed to air-dry before a volume of 1 μL of sinapinic acid solution [50% sinapinic acid saturated in 30% (v/v) acetonitrile 10% isopropyl alcohol and 0.5% in TFA] was applied to each spot twice. The array was air-dried between each application. PCS 4000 Enterprise SELDI-TOF-MS (Bio-Rad) was used to obtain the mass of the sample components.

Circular dichroism (CD)

Far-UV CD spectra were collected from 185 to 260 nm on a Jasco 810 spectropolarimeter using a 1 mm path length quartz cuvette at 20°C. CD measurements were recorded for untreated α-syn monomer (0.074 mg/mL), Met-oxidised α-syn monomer (0.070 mg/mL), α-syn:DA dimer (0.127 mg/mL) and α-syn:DA trimer (0.15 mg/mL) in 10 mM sodium phosphate at pH 7.4. Baseline spectra acquired for buffer without α-syn and DA were subtracted. Secondary structure analysis was performed using CDSSTR deconvolution on the DICHROWEB website located at http://dichroweb.cryst.bbk.ac.uk, which is supported by grants to the BBSRC Centre for Protein and Membrane Structure and Dynamics (CPMSD) (Lobley et al. 2004; Whitmore and Wallace 2004, 2008). To verify SAXS sample stability, far-UV CD spectra were measured parallel to (without irradiation) and immediately after SAXS experiments using a Jasco 815 spectropolarimeter in 0.1 mm path length quartz cell (Hellma) at 4°C.

Electron paramagnetic resonance (EPR) spectroscopy

EPR experiments were carried out at X-band (ca. 9.4 GHz) with a Bruker ESP380E CW/FT spectrometer. The measurements were made at sample temperatures of 297 and 77 K using the standard rectangular TE_{102} cavity and a quartz cold finger Dewar insert. At both temperatures, 50 μL of sample was contained in a quartz tube. Microwave frequencies were measured with an EIP Microwave 548A frequency counter.

Small angle X-ray scattering (SAXS)

SAXS data were acquired on a Bruker SAXS NanoSTAR three-pinhole collimation instrument with a rotating anode source (wavelength Cu Kα $\lambda = 1.5418$ Å) with a Bruker Vantec 2D detector (sample-to-detector distance 700 mm, resolution 100 μm). SAXS data were acquired for α-syn samples at 4°C. Protein sample stability was verified by the unchanging CD profile (not shown) of the samples before and after SAXS experiments. Further, extended SAXS collection in hourly increments showed no change in scattering data. Radial averaging to produce 1D-scattering intensity profiles of $I(q)$ vs. q for a q range ≈ 0.02–0.3 Å^{-1} (where the scattering vector $q = 4\pi \sin(\theta)/\lambda$ and 2θ is the scattering angle) was done using Bruker SAXS data collection software, which includes corrections for detector sensitivity. Data analysis and modelling were carried out using appropriate members of the ATSAS suite of programs, available from http://www.embl-Hamburg.de/ExternalInfo/Research/Sax/index.html. The program PRIMUS (Konarev et al. 2000) was used to perform solvent blank subtractions and Guinier analysis. GNOM was used to obtain distance distribution functions; DAMMIF (Franke and Svergun 2009) for restoring ab initio low resolution shape as a space-fill assembly of 'dummy atoms' from the isotropic scattering data; GASBOR for ab initio reconstruction as a chain of 'dummy residues', and CRYSOL for evaluating the scattering curves from GASBOR models (Svergun and Koch 2002).

Results

Size fractionation of α-syn:DA species

SDS-PAGE analysis of α-syn incubated in the absence and presence of DA showed a distinct oligomeric banding pattern for the samples incubated with DA (Fig. 1a), representing monomer, dimer, trimer and higher molecular weight oligomers. The α-syn:DA species were separated according to their molecular mass by SEC as described in the "Experimental" section. Figure 1b shows the SEC elution profile of the α-syn:DA oligomers. The solution colour of eluted fractions at the start of peak 1 from the elution profile was dark brown. This brownish solution colour was lighter for eluted fractions toward the end of peak 1. A slight brown tint was observed in the eluted fractions from peak 2, with a near colourless solution observed for eluted fractions from peak 3. The brown colour observed in the solution of the eluted fractions indicated the presence of polymeric DA, known as melanin. SDS-PAGE analysis of the eluted fractions (Fig. 2) revealed the first peak from the elution profile to consist of HMW oligomers. The shoulder between peak 1 and peak 2 from the elution profile indicated the presence of trimeric and tetrameric species. The second peak from the elution profile represented the dimeric species, while the third peak was of monomeric species. A protein band was not detected on the SDS-PAGE of the eluted fraction for peak 4 containing mainly polymeric DA.

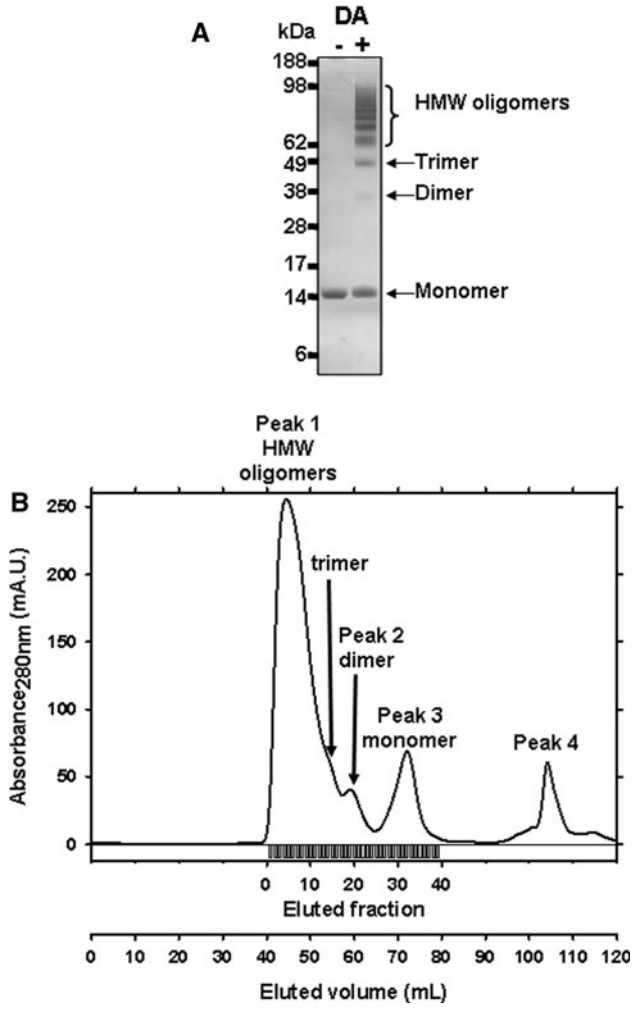

Fig. 1 Size exclusion chromatography of α-syn:DA soluble oligomers. **a** SDS-PAGE analysis of the soluble fractions of α-syn incubated in the absence and presence of DA following high speed centrifugation. **b** SEC elution profile of α-syn:DA oligomers. Soluble fractions of α-syn:DA oligomers were loaded onto a HiLoad Superdex 200 16/60 s column. The oligomers were eluted at a flow rate of 1 mL/min, and 1 mL fractions were collected as indicated on the figure

Sedimentation velocity analysis (SVA) of α-syn:DA species

The sedimentation behaviour of a molecule in solution is dependent on the size and the shape of the molecule. To determine the size distribution of selected SEC fractions, samples were subjected to SVA and the sedimentation rate of molecules in solution was monitored over a period of 16 h by collecting the absorbance scan along the radius of the centrifuge cell. These scans were fitted to the c(M) model (Schuck 2000). Figure 3 shows the molar mass distribution of the HMW and LMW oligomer fractions. The results from the SVA are summarised in Table 1. The size distribution of the HMW oligomers (Fig. 3a) was much broader than that of the LMW oligomers (Fig. 3b), indicating a greater polydispersity of the HMW samples. There was a decrease in the polydispersity as the oligomers eluted from the SEC column. The size distribution was broad in the fractions toward the start of peak 1 and much narrower in the fractions toward the end of peak 1 (i.e. compare the size distribution of fraction 3 to fraction 8). The size distributions of the LMW oligomers (Fig. 3b) were much more defined, with a sharp, narrow size distribution observed for the monomeric samples (fraction 31 and the untreated α-syn monomer). It should be noted that fraction 31 of SEC is the monomeric α-syn species. According to electrospray mass spectrometry, the average mass for this species was 14,524 Da, corresponding to the mass of monomeric α-syn with four oxidised Met (data not shown), consistent with previous observations (Leong et al. 2009b; Pham et al. 2009). Hereafter, we refer to this monomeric species as Met-oxidised α-syn monomer. The narrow size distribution of the LMW oligomer fractions indicated that these fractions were monodisperse. It can be seen from Table 1 that all fractions, with the exception of the monomer, have molecular masses exceeding that expected for the modal subunit of α-syn, most likely bound to DA. From Table 1, the excess MW due to DA is approximately 3 kDa, equivalent to 20 DA molecules for every additional α-syn molecule added to the dimer. Indeed, MALDI TOF analysis of the dimeric and trimeric fractions indicated a mass of 32,244 and 49,707 Da respectively. These masses corresponded to addition of 3,324 Da (22 DA molecules) for the dimer and 6,327 Da (42 DA molecules) for the trimer (Fig. 4).

In analysing the sedimentation velocity data using the c(M) model, the weight-average frictional ratio (f/f_0) was assumed to be the same for all the species in a given sample. The frictional ratio reflects the shape of the protein in solution; it is a measure of sphericity of the molecule. For a globular protein, $f/f_0 < 1.25$ and for a non-globular protein with an extended conformation $f/f_0 > 1.25$ and depends on the size of the protein. From the results of the SVA of α-syn:DA species, the fitted frictional ratio for all oligomer fractions was in the range 1.8–2.5 (Table 1), indicating that the oligomers may have an extended or asymmetric conformation.

Circular dichroism of α-syn:DA species

CD spectra of the α-syn:DA oligomers were characterised by a negative minimum in the vicinity of 200 nm (Fig. 5), which indicated that their secondary structure is largely random coil as was the case with the untreated α-syn monomer and Met-oxidised α-syn monomers. The CDSSTR deconvolution profiles ($n > 3$) of untreated and Met-oxidised α-syn monomer were essentially identical, i.e. there was no change in regular secondary structure elements such as α-helix and β-sheet content upon exposure to DA

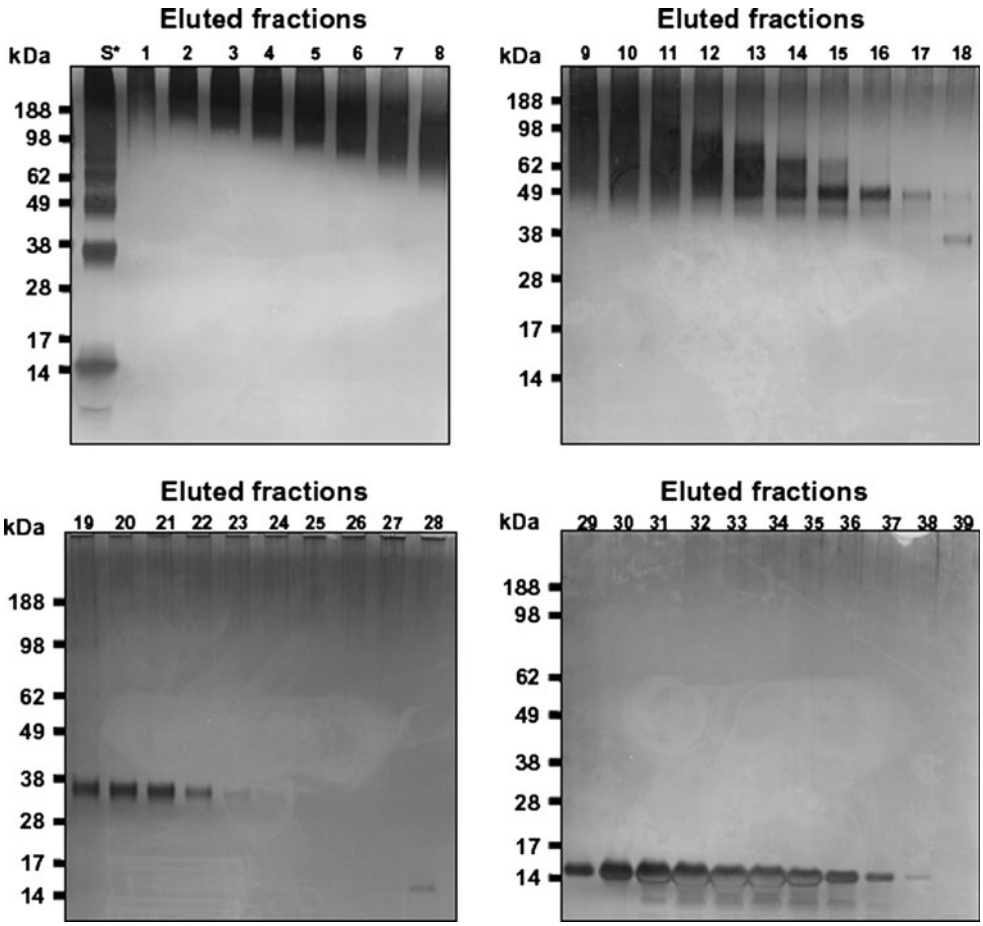

Fig. 2 SDS-PAGE/silver stained analysis of the eluted fractions from SEC of soluble α-syn:DA oligomers (as shown in Fig. 1b)

(Table 2). On the other hand, DA-induced oligomerisation caused a decrease in random coil conformation as indicated by the loss of negative minimum at 200 nm (Fig. 5). Deconvolution of the α-syn:DA dimer and trimer CD spectra showed similar secondary structural elements for both of these oligomeric species with an increase in the β-sheet and turns content and a decrease in the unordered conformation relative to the monomer (Table 2).

EPR spectroscopy of α-syn:DA species

In view of the dark colour observed in the SEC fractions suggesting the presence of melanins, these fractions were examined by EPR spectroscopy. In no case was a melanin radical at $g = 2.0034$ detected at either 77 or 297 K, suggesting that any quinone reaction products of the DA had reacted with the α-syn, supporting the conclusions from our data of SVA and mass spectrometry and earlier studies (Conway et al. 2001).

SAXS comparison of α-syn:DA samples

SAXS experiments were performed for selected eluted fractions from SEC (Fig. 1b). Analysis of SAXS data showed that the radius of gyration, R_g, progressively increased from 371 ± 1 Å for fraction 31 to 105 ± 2 Å for fraction 3 (Table 1). At the same time, the SAXS curves for these species indicated an increasing globularisation as the modal mass increased, reflected by the shape of Kratky plots, q vs. $q^2I(q)$, (Fig. 6a). A scattering curve in the Kratky plot has a characteristic maximum for globular-shaped molecules, while for 'linear' molecules, e.g. unfolded proteins, such a maximum is absent from the Kratky plot (Glatter and Kratky 1982), as previously shown for α-syn (Uversky et al. 2001). These data are consistent with electron micrographs of α-syn oligomers treated with DA, which showed roughly globular species (Cappai et al. 2005).

SAXS of untreated α-syn and the monodisperse α-syn:DA fractions (monomer and trimer)

As indicated by the SVA data (Fig. 3), the monomeric (fraction 31 from SEC) and trimeric (fraction 16) α-syn samples were monodisperse, thus we chose these fractions for detailed SAXS analysis. The fitted SAXS data, collected at a concentration of 12.9 mg/mL for Met-oxidised α-syn monomer (fraction 31) had an $R_g = 37 \pm 1$ Å

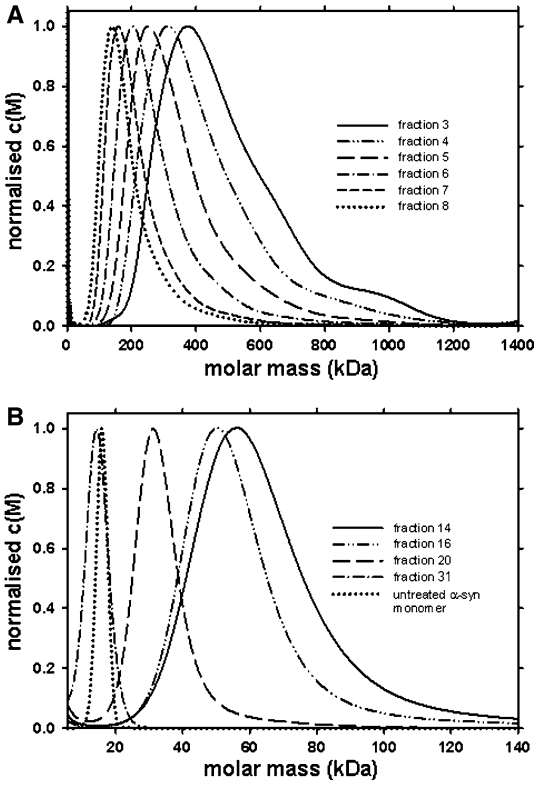

Fig. 3 Continuous molar mass distribution of α-syn:DA oligomers. Selected fractions of HMW (**a**) and LMW (**b**) α-syn:DA oligomers from SEC were subjected to SVA as described in the "Experimental" section

(Guinier analysis). This was consistent with the values obtained for untreated α-syn monomer (36 ± 1 and 34 ± 1 Å at 6.9 and 1.7 mg/mL, respectively), meaning that the presence of DA did not affect α-syn monomer's conformation. These values were also within the range expected for a 140 residue unfolded protein in a close to ideal solvent (~38 Å) (Kohn et al. 2004). The α-syn:DA trimer (fraction 16) at a concentration of 1.1 mg/mL had an $R_g = 50 \pm 3$ Å. This value for the trimer was too low to be accounted for by the relationship between R_g and the number of residues (N), $R_g = R_0 N^v$, where $v = 0.588$ for a real, excluded-volume random coil polymer and R_0 is a constant dependent on the persistence length of the polymer [$R_0 = 2.1$ Å (Plaxco and Dobson 1996)]. The expected R_g for three end-to-end associated random coil α-syn molecules would be around 70 Å. This discrepancy could be accounted for by the existence of cross-links between the chains and/or some degree of structuring in the α-syn:DA trimer. Kratky plots of the SAXS data of Met-oxidised α-syn monomer and α-syn:DA trimer (Fig. 6b) indicated that both species had non-globular shape. Consistently, the distance distribution P(r) functions (Fig. 6c) obtained by the inverse Fourier transformation of the SAXS profile indicated that untreated monomer, Met-oxidised α-syn monomer and α-syn:DA trimer had elongated shapes with maximum dimensions $D_{max} = 130$, 150 and 170 Å respectively (Fig. 6c).

Subsequent ab initio modelling using DAMMIF software produced a number of models for untreated α-syn, Met-oxidised α-syn monomer and α-syn:DA trimer.

A new approach to define the representative structure among all equally probably solutions given by DAMMIF [personal communication with Maxim V. Petoukhov, Biological Small Angle Scattering Group, EMBL, Hamburg Outstation, Germany] was used. The new algorithm organises the given set of DAMMIF solutions into clusters based on their similarity using a normalised spatial discrepancy (Kozin and Svergun 2001) as a figure of merit. Then structures within each cluster are averaged to build the

Table 1 SEC data, molecular mass and frictional ratios for size exclusion column fractions of DA-treated α-syn

Eluted fraction	Frictional ratio (f/f_0)	Modal mass (kDa)	Modal subunit α-syn	Radius of gyration (Å)
Fr. 3	2.39	374.13	25.80	105 ± 2
Fr. 4	2.44	318.60	21.97	88± 1
Fr. 5	2.45	253.50	17.48	–
Fr. 6	2.37	205.11	14.15	–
Fr. 7	2.25	160.27	11.05	78 ± 1
Fr. 8	2.26	139.27	9.60	67± 1
Fr. 10	–	–	–	61 ± 1
Fr. 11	–	–	–	55 ± 1
Fr. 12	–	–	–	52 ± 1
Fr. 14	1.98	54.50	3.77	44 ± 1
Fr. 16 (α-syn:DA trimer)	2.00	49.48	3.42	50 ± 1
Fr. 20 (α-syn:DA dimer)	1.85	31.14	2.15	40 ± 2
Fr. 31 (Met-ox monomer)	1.87	14.22	0.98	37± 1
Untreated monomer	1.95	15.87	1.10	36± 1

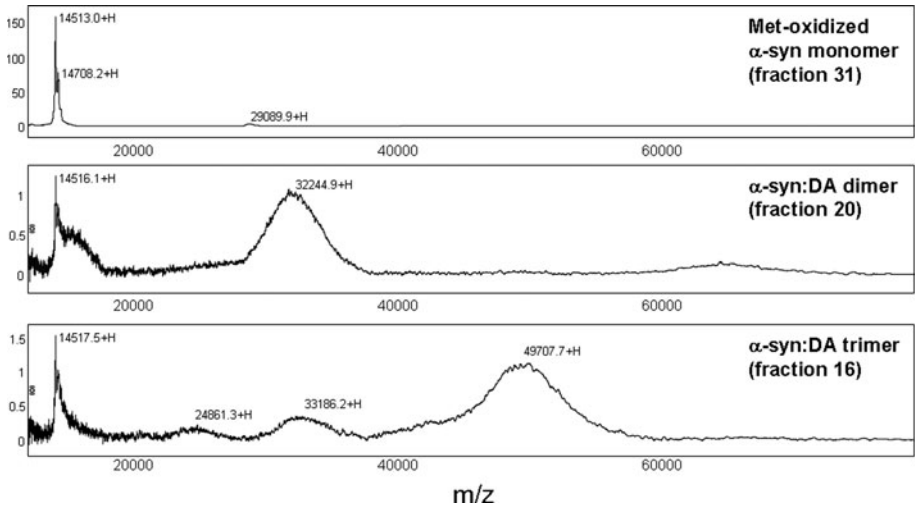

Fig. 4 MALDI-TOF spectra of Met-oxidised α-syn monomer, α-syn:DA dimer and trimer

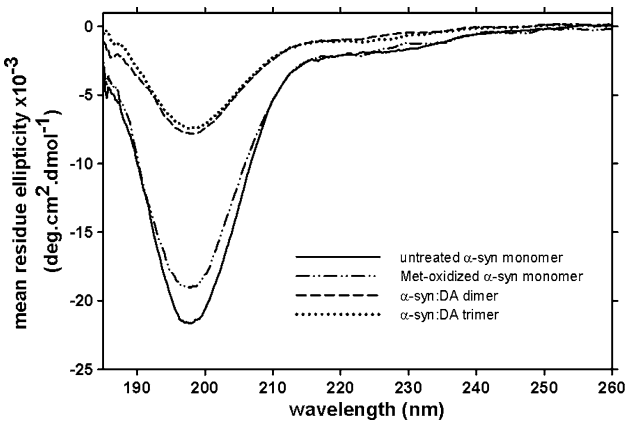

Fig. 5 CD spectra of untreated monomer, Met-oxidised α-syn monomer and α-syn:DA dimer and trimer, acquired in parallel to SAXS measurements

representative structure(s). For the simple globular shapes the algorithm yields one structure whose shape represents the most probable model for the protein in solution. In the case of more complicated or flexible particle envelopes, the new approach generates a set of equally probable shapes.

Figure 7 shows representative sets of ab initio restored elongated shapes for untreated α-syn (Fig. 7a), for Met-oxidised α-syn monomer (Fig. 7b) and for the α-syn:DA trimer (Fig. 7c), with anisometry ratios of ca. 5.3:1 for both Met-oxidised α-syn monomer and α-syn:DA trimer or ca. 3:1 for their envelopes. The worm-like shapes of the depicted molecules were therefore reasonable solutions for DAMMIF modelling from the mathematical point of view, as according to Volkov and Svergun (2003), shapes with anisometry of up to 1:10 can be restored from their SAXS curves.

The longest distances in .pdb coordinate files of Met-oxidised α-syn monomer and α-syn:DA trimer models were 133 ± 3 and 163 ± 1 Å respectively. These dimensions suggested that the α-syn:DA trimer consisted of approximately parallel, aligned monomers, although with some degree of overlap or folding. Models of monomers (untreated and Met-oxidised) showed a high degree of similarity and their shape was always asymmetric—a worm-like species with a 'head' and 'tail' ends (Fig. 7a,b). The models of trimer were more so, indicating that one end of the molecule may be less well defined than the other end (Fig. 7c). It is possible then that the α-syn:DA trimer population contained a mixture of species with different modes of assembly.

Another ab initio modelling approach of Met-oxidised α-syn monomer and α-syn:DA trimer using the GASBOR program, which, contrary to DAMMIF, utilises the high-q data portion, yielded chain-like structures composed of dummy residues. Careful inspection of possible alignment configurations of partly structured monomers allowed the construction of a model of the trimer from three model units of the monomer. These are shown in Fig. 8a. Direct alignment of monomer models within a trimer did not produce a reasonable fit, however when the monomer structures were 'bent in the middle' they could be superimposed onto the trimer structure. This suggests that some structuring of α-syn occurred upon α-syn:DA trimer formation, consistent with our CD data. A SAXS curve for this construct was computed using the CRYSOL program and it showed good agreement ($\chi = 0.985$) with the α-syn:DA trimer SAXS data (Fig. 8b).

Discussion

The molecular mass from MALDI-TOF and SVA, and the EPR data suggested that α-syn monomers were cross-linked with polymeric DA species (melanin) within the oligomers. It has already been shown that DA and its reactive intermediates oxidise all four Met residues in

Table 2 Structural characteristics of monomeric, dimeric and trimeric α-syn

	α-Helix	β-Sheet	Turns	Unordered
Untreated α-syn monomer	0.02 ± 0.03	0.11 ± 0.07	0.08 ± 0.07	0.78 ± 0.15
Met-ox monomer (fr. 31)	0.01 ± 0.02	0.13 ± 0.06	0.08 ± 0.06	0.76 ± 0.13
α-syn:DA dimer (fr. 20)	0.01 ± 0.02	0.31 ± 0.08	0.16 ± 0.07	0.49 ± 0.11
α-syn:DA trimer (fr.16)	0.02 ± 0.02	0.31 ± 0.06	0.21 ± 0.11	0.44 ± 0.14

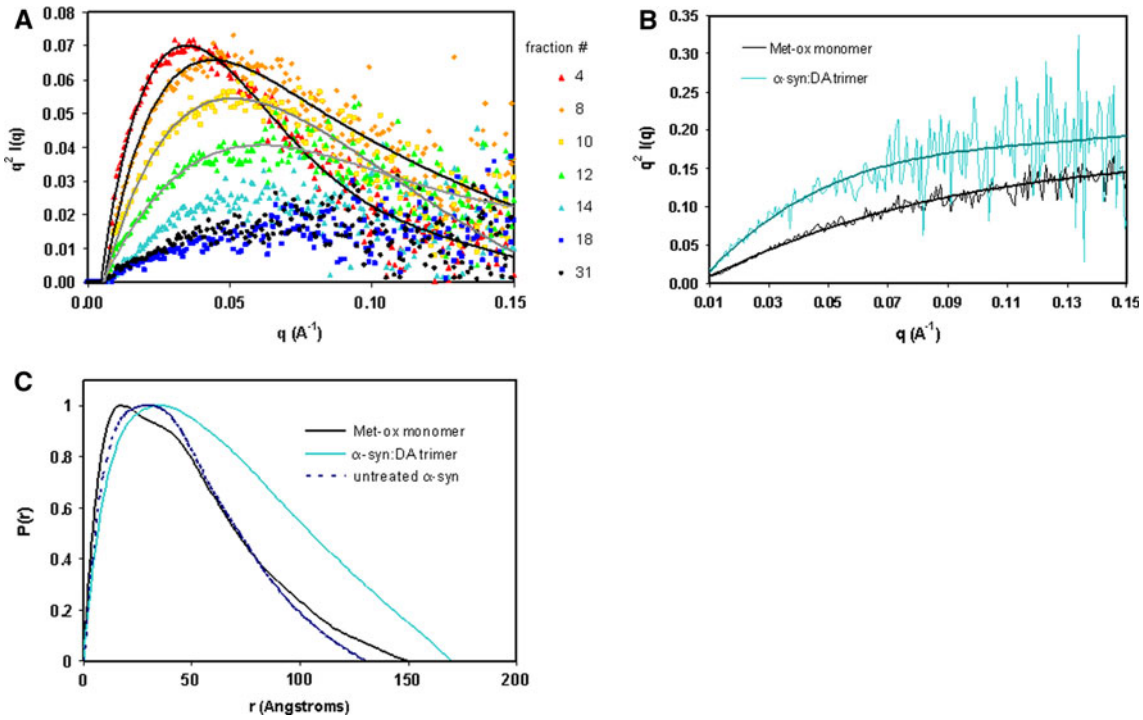

Fig. 6 SAXS data for Met-oxidised α-syn monomer. **a** Kratky plots for selected DA-induced α-syn oligomers of HMW and LMW. Polynomial (4th order) curves (*solid lines*) were fitted to the datasets of fractions 4, 8, 10 and 12 in order to distinguish them at higher q values where significant data overlap occurs. **b** Kratky plot of Met-oxidised α-syn monomer and α-syn:DA trimer. **c** Plot of distance distribution function P(r) of Met-oxidised α-syn monomer and α-syn:DA trimer

monomeric α-syn, which with time associate to form α-syn oligomeric species (Conway et al. 2001; Li et al. 2004; Norris et al. 2005; Cappai et al. 2005; Leong et al. 2009a, b). Our SAXS and CD data showed that Met-oxidised α-syn monomers are elongated worm-like shapes, similar to monomeric untreated α-syn, lacking significant secondary structure elements, whereas the α-syn:DA dimers and trimers appeared to have more β-sheet and turn content. The shape of trimers was less defined than that of monomers; however their size indicated that monomers tended to be aligned side-by-side with partial overlap rather than associated via end-to-end interactions. Despite increased propensity for β-sheet formation (Table 2), this arrangement of monomers in small oligomers may prevent ordered lateral association of α-syn molecules typical of fibrillisation. The increasing frictional ratio and R_g values (Table 1) showed that as the α-syn:DA oligomers increased in size, their shape became more globular, but no evidence of more secondary structure was found in those species (CD data not shown).

The shape of monomeric α-syn in solution

Our data suggested that untreated monomeric α-syn assumed a partly extended form in solution. We have two indicators of the lack of structure for the untreated and Met-oxidised α-syn monomer. These are their frictional ratios >1.25 and CD data (Tables 1 and 2). However, in relation to the latter we need to recall the observations of Fitzke and Rose (2004) who showed that a protein could behave as a random coil even if it contains non-random segments, provided they are linked by backbone residues whose torsion angles have been varied at random. The occurrence of structured regions in monomeric native α-syn has been suggested in a number of earlier studies (Kohn et al. 2004; Bertoncini et al. 2005). Our R_g values of untreated α-syn

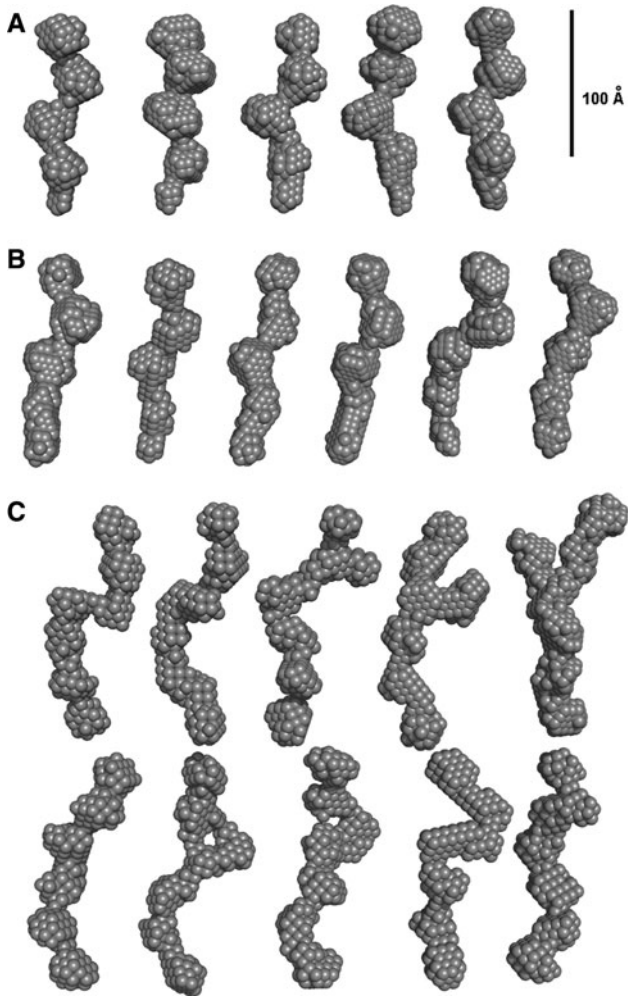

Fig. 7 Ab initio models of **a** untreated α-syn, **b** Met-oxidised α-syn monomer and **c** α-syn:DA trimer built by DAMMIF software. Each model is a probability-equivalent averaged solution by clustering. The 100 Å *scale bar* applies to all panels

monomer, which fitted into the power law for an unfolded protein of a slightly shorter length (~120 residues), indicated that this molecule had some residual structure.

The shape of α-syn:DA trimers in solution

Our CD spectra showed that, as in the case of the monomer, the α-syn:DA dimer and trimer possessed a largely unstructured conformation. Our SAXS reconstructions of the trimers showed that the worm-like shape was retained giving the appearance of overlapping monomers with no end-to-end association. This finding appeared to be different from the previously published conformations of α-syn oligomers obtained under different experimental conditions. For example, in a study of fibril formation occurring during prolonged incubation in the absence of DA, Tashiro et al. (2008) used 2D ^{1}H-^{15}N NMR spectroscopy, electron microscopy and SAXS to investigate the structural properties and propensities to form fibrils of α-syn at the initial stage. Observation of the ^{1}H-^{15}N HSQC spectra indicated significant attenuation of many cross peak intensities in the regions of the KTKEGV-type repeats located in or near the NAC (non-amyloid component) region of α-syn, suggesting that these regions contributed to fibril formation (Tashiro et al. 2008). In other studies not involving DA, atomic force and electron microscopy showed that the oligomers formed by either wild-type or mutant α-syn had a number of different morphologies including spherical, chain-like, ring-like and annular structures (Conway et al. 2000; Lashuel et al. 2002). Further, an important property of the DA-induced oligomers is their low β-sheet content (Cappai et al. 2005 and Table 2), which contrasts with that reported for α-syn fibrils, where a continuous middle segment contains systematically H-bonded β-structure (Heise et al. 2005; Del Mar et al. 2005). In addition, Fukuma et al. (2008), using frequency modulation atomic force microscopy, were able to show individual β-strands with a spacing of 5 Å that were aligned perpendicular to the fibril axis.

The nature of the molecular association in the oligomers

Although we cannot completely exclude the possibility that DA melanin cross-links the monomers through tannin-like hydrophobic and electrostatic interactions, it is known that DA-quinone reacts with α-syn by coupling its Tyr residues and by nucleophilic attack on Lys residues forming a Schiff base (Conway et al. 2001). Our MW data from SVA (Table 1) and MALDI TOF mass spectrometry (Fig. 4) suggested that there was a stochiometric interaction between α-syn and DA polymers. The relationship between DA and α-syn can be expressed as modal mass = $n \times$ MW α-syn + $(n - 1) \times 4.8$ kDa, where n is the number of α-syn molecules in the oligomer. The mass of 3 kDa represented addition of approximately 20 DA quinones per α-syn molecule, suggesting that it reacts with all of the 15 Lys residues and the 5 Tyr residues. The distribution of these residues in the sequence is shown in Fig. 9a. This relationship implied that DA was cross-linking α-syn while polymerising to form melanin. A way in which the Lys residues of the imperfect KXKXX repeats could be linked is shown in Fig. 9b. We did not see an EPR signal characteristic of unbound melanin, giving support to the cross-linking hypothesis. However, even though cross-linking may explain the α-syn lateral association seen in the trimers, it would not be a sufficient explanation for the inhibition of fibril formation: such cross linking could still lead to fibril formation, albeit of a different kind. In fact, a prolonged incubation of α-syn with equimolar amount of DA eventually led to formation of fibrils (Follmer et al. 2007). Although their structural parameters were not investigated,

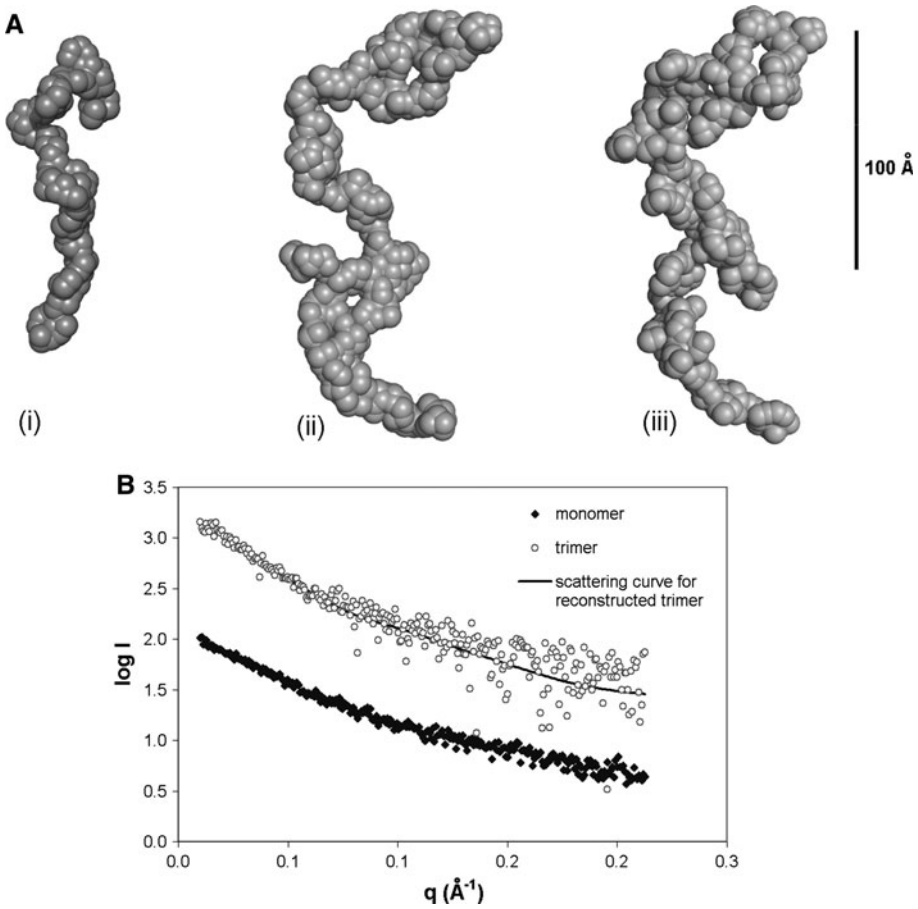

Fig. 8 A representative reconstruction of an α-syn:DA trimer from three models of the monomer. **a** *i* Ab initio models for monomer restored by GASBOR. *ii* Ab initio models for trimer restored by GASBOR. *iii* Plausible model of the trimer constructed by superimposing three modified ab initio monomer's structures. **b** Scattering pattern from plausible model of trimer shown on panel (**a**, *iii*), computed using CRYSOL

these fibrils were unstable and susceptible to breakage. The authors hypothesize that fibril degradation to protofibril-size species may be responsible for cytotoxic effect of DA and neuronal loss.

The role of DA oxidation in inhibiting fibril formation

The importance of intact N- and C-terminal fragments of α-syn in modulating fibril formation was indicated by studies on α-syn truncated forms. Removal of the first 60 residues caused rapid fibrillisation, albeit with different CD spectral profile (Rekas et al. unpublished), while naturally occurring C-terminally truncated species stimulate aggregation of full-length α-syn (Liu et al. 2005). Qin et al. (2007) used α-syn mutants lacking C- and N-termini to show that these were not involved in soluble protofilament formation but played a key part in the resulting fibril structure. In the case of DA-treated α-syn, there was evidence that the Met residues at both the N-terminal (M1, M5) and the C-terminal (M116, M127) ends of the molecule were oxidised (Leong et al. 2009a, b), which would markedly increase the polarity of these regions. Such an increase in polarity could weaken hydrophobic interactions between the ends of the chains and reduce end-to-end associations in the process of fibrillisation. Presumably, the observation that DA and L-dopa can disaggregate α-syn fibrils (Li et al. 2004) could be explained by their involvement in oxidation of the Met residues, again weakening the end-of-chain interactions. It should be noted that mild hydrogen peroxide treatment also oxidised the α-syn Met residues (Glaser et al. 2005) and inhibited fibrillisation (Leong et al. 2009a). In this case, it was found that the inhibition was proportional to the number of oxidised residues.

Oligomers and neurotoxicity

There is yet no evidence that α-syn:DA oligomers are toxic when added to cultures of neuronal cells, in contrast to oligomers prepared in other ways (Karpinar et al. 2009; Kim et al. 2009) and the well-documented toxicity of oligomers in AD or the prion diseases (Barnham et al. 2006). However, Ito et al. (2010) suggested that the coexistence of human α-syn with catecholamine enhanced the endoplasmic reticulum stress-related toxicity in PD pathogenesis. They found that addition of thapsigargin, a sesquiterpene lactone inhibitor of sarco/endoplasmic reticulum Ca^{2+} ATPase, to PC12 cells expressing human α-syn increased the SDS soluble oligomers of α-syn associated with

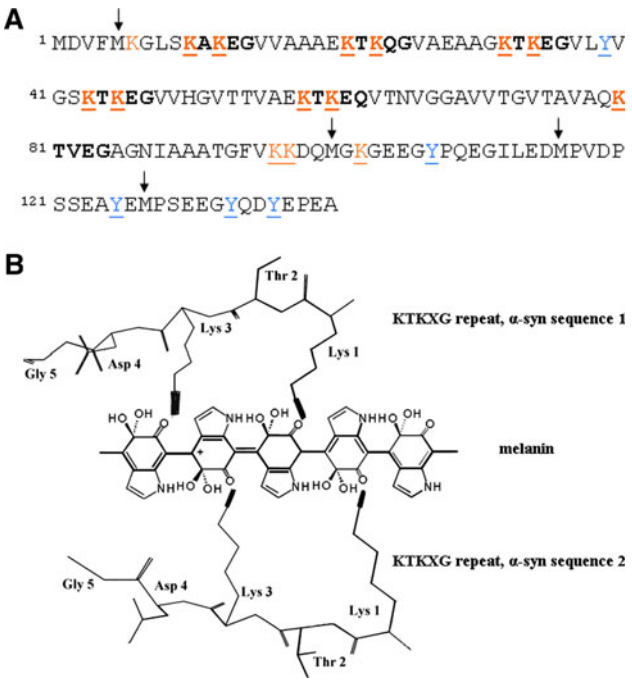

Fig. 9 Proposed model of interaction of α-syn with DA. **a** Amino acid sequence of α-syn, showing the distribution of Lys and Tyr residues that could react with dopamine-derived quinones. **b** Cartoon showing potential quinone interaction with the Lys residues of the KTKXG imperfect repeats in the N-terminal region of α-syn

catecholamine-quinone. They also found that thapsigargin increased eIF2alpha phosphorylation and nuclear GADD153/CHOP induction under conditions of α-syn over-expression. Transgenic PARK 1 mice have been available for some time (Chesselet 2008) and it would be of interest to construct these with mutants lacking the Lys and Tyr residues that might be important in the reaction with DA and to see if these animals suffered from dopaminergic neuron loss compared with those over-expressing wild-type human α-syn.

The major metabolite of the neurotoxic psychostimulant ethylenedioxymethamphetamine (MDMA, ecstasy) is the 3,4-dihydroxymethamphetamine derivative (HHMA), which is easily oxidisable to the orthoquinone species. This can participate in redox cycling, generating reactive oxygen species (ROS) and semiquinone radicals which could react to cross-link α-syn in the manner suggested for DA. Recently, a unifying theme for the toxicity of other psychostimulants, such as methamphetamine (METH) was proposed based on electron transfer, ROS and oxidative stress (Kovacic 2005). This would suggest that the current interest in therapeutic approaches to treating PD and the consequences of exogenous neurotoxic insults by blocking quinone formation (Miyazaki and Asanuma 2009) should include quinone interactions with α-syn.

Acknowledgments The authors would like to thank AINSE Ltd for providing financial assistance (award no. AINGRA09043) to enable the SAXS study to be conducted. The other studies in this work were supported by a Program Grant from the National Health and Medical Research Council of Australia NHMRC), the Neuroproteomic and Neurogenomic Facility and a grant under The University of Melbourne-ANSTO Collaborative Agreement. K.J.B. and R.C. are NHMRC Senior Research Fellows. Instruments at the National Deuteration Facility were partly funded by the National Collaborative Research Infrastructure Strategy of the Australian Government. The authors acknowledge the Research Transfer Facility at Bio21 Molecular Science and Biotechnology Institute, The University of Melbourne for assistance with electrospray mass spectrometry performed in the course of this research.

References

Barnham KJ, Cappai R, Beyreuther K, Masters CL, Hill AF (2006) Delineating common molecular mechanisms in Alzheimer's and prion diseases. Trends Biochem Sci 31:465–472

Bertoncini CW, Jung YS, Fernandez CO, Hoyer W, Griesinger C, Jovin TM, Zweckstetter M (2005) Release of long-range tertiary interactions potentiates aggregation of natively unstructured alpha-synuclein. Proc Natl Acad Sci USA 102:1430–1435

Burke WJ, Kumar VB, Pandey N, Panneton WM, Gan Q, Franko MW, O'Dell M, Li SW, Pan Y, Chung HD, Galvin JE (2008) Aggregation of alpha-synuclein by DOPAL, the monoamine oxidase metabolite of dopamine. Acta Neuropathol 115:193–203

Cappai R, Leck SL, Tew DJ, Williamson NA, Smith DP, Galatis D, Sharples RA, Curtain CC, Ali FE, Cherny RA, Culvenor JG, Bottomley SP, Masters CL, Barnham KJ, Hill AF (2005) Dopamine promotes alpha-synuclein aggregation into SDS-resistant soluble oligomers via a distinct folding pathway. Faseb J 19:1377–1379

Chesselet MF (2008) In vivo alpha-synuclein overexpression in rodents: a useful model of Parkinson's disease? Exp Neurol 209:22–27

Conway KA, Lee SJ, Rochet JC, Ding TT, Williamson RE, Lansbury PT Jr (2000) Acceleration of oligomerization, not fibrillization, is a shared property of both α-synuclein mutations linked to early-onset Parkinson's disease: implications for pathogenesis and therapy. Proc Natl Acad Sci USA 97:571–576

Conway KA, Rochet JC, Bieganski RM, Lansbury PT Jr (2001) Kinetic stabilization of the α-synuclein protofibril by a dopamine-α-synuclein adduct. Science 294:1346–1349

Del Mar C, Greenbaum EA, Mayne L, Englander SW, Woods VL Jr (2005) Structure and properties of alpha-synuclein and other amyloids determined at the amino acid level. Proc Natl Acad Sci USA 102:15477–15482

El-Agnaf OM, Jakes R, Curran MD, Wallace A (1998) Effects of the mutations Ala^{30} to Pro and Ala^{53} to Thr on the physical and morphological properties of α- synuclein protein implicated in Parkinson's disease. FEBS Lett 440:67–70

Fitzke NC, Rose GD (2004) Reassessing random-coil statistics in unfolded proteins. Proc Natl Acad Sci USA 101:12497–12502

Follmer C, Romão L, Einsiedler CM, Porto TC, Lara FA, Moncores M, Weissmüller G, Lashuel HA, Lansbury P, Neto VM, Silva JL, Foguel D (2007) Dopamine affects the stability, hydration, and packing of protofibrils and fibrils of the wild type and variants of alpha-synuclein. Biochemistry 46(2):472–482

Franke D, Svergun DI (2009) *DAMMIF*, a program for rapid ab-initio shape determination in small-angle scattering. J Appl Cryst 42:342–346

Fukuma T, Mostaert AS, Serpell LC, Jarvis SP (2008) Revealing molecular-level surface structure of amyloid fibrils in liquid by

means of frequency modulation atomic force microscopy. Nanotechnology 19:84010
Glaser CB, Yamin G, Uversky VN, Fink AL (2005) Methionine oxidation, alpha-synuclein and Parkinson's disease. Biochim Biophys Acta 1703:157–169
Glatter O, Kratky O (1982) Small angle X-ray scattering. Academic Press, New York, p 115
Heise H, Hoyer W, Becker S, Andronesi OC, Riedel D, Baldus M (2005) Molecular-level secondary structure, polymorphism, and dynamics of full-length α-synuclein fibrils studied by solid-state NMR. Proc Natl Acad Sci USA 102:15871–15876
Ito S, Nakaso K, Imamura K, Takeshima T, Nakashima K (2010) Endogenous catecholamine enhances the dysfunction of unfolded protein response and alpha-synuclein oligomerization in PC12 cells overexpressing human alpha-synuclein. Neurosci Res 66:124–130
Karpinar DP, Balija MB, Kugler S, Opazo F, Rezaei-Ghaleh N, Wender N, Kim HY, Taschenberger G, Falkenburger BH, Heise H, Kumar A, Riedel D, Fichtner L, Voigt A, Braus GH, Giller K, Becker S, Herzig A, Baldus M, Jackle H, Eimer S, Schulz JB, Griesinger C, Zweckstetter M (2009) Pre-fibrillar alpha-synuclein variants with impaired beta-structure increase neurotoxicity in Parkinson's disease models. EMBO J 28:3256–3268
Kim HY, Cho MK, Kumar A, Maier E, Siebenhaar C, Becker S, Fernandez CO, Lashuel HA, Benz R, Lange A, Zweckstetter M (2009) Structural properties of pore-forming oligomers of alpha-synuclein. J Am Chem Soc 131:17482–17489
Kohn JE, Millett IS, Jacob J, Zagrovic B, Dillon TM, Cingel N, Dothager RS, Seifert S, Thiyagarajan P, Sosnick TR, Hasan MZ, Pande VS, Ruczinski I, Doniach S, Plaxco KW (2004) Random-coil behavior and the dimensions of chemically unfolded proteins. Proc Natl Acad Sci USA 101:12491–12496
Konarev PV, Volkov VV, Sokolova AV, Koch MHJ, Svergun DI (2000) PRIMUS: a Windows PC-based system for small-angle scattering data analysis. J Appl Cryst 36:1277–1282
Konarev PV, Petoukhov MV, Volkov VV, Svergun DI (2006) ATSAS 2.1, a program package for small-angle scattering data analysis. J Appl Cryst 39:277–286
Kovacic P (2005) Unifying mechanism for addiction and toxicity of abused drugs with application to dopamine and glutamate mediators: electron transfer and reactive oxygen species. Med Hypotheses 65:90–96
Kozin MB, Svergun DI (2001) Automated matching of high- and low-resolution structural models. J Appl Cryst 34:33–41
Lashuel HA, Petre BM, Wall J, Simon M, Nowak RJ, Walz T, Lansbury PT Jr (2002) α-Synuclein, especially the Parkinson's disease-associated mutants, forms pore-like annular and tubular protofibrils. J Mol Biol 322:1089–1102
Leong SL, Cappai R, Barnham KJ, Pham CL (2009a) Modulation of alpha-synuclein aggregation by dopamine: a review. Neurochem Res 34:1838–1846
Leong SL, Pham CL, Galatis D, Fodero-Tavoletti MT, Perez K, Hill AF, Masters CL, Ali FE, Barnham KJ, Cappai R (2009b) Formation of dopamine-mediated alpha-synuclein-soluble oligomers requires methionine oxidation. Free Radic Biol Med 46:1328–1337
Li J, Zhu M, Manning-Bog AB, Di Monte DA, Fink AL (2004) Dopamine and L-dopa disaggregate amyloid fibrils: implications for Parkinson's and Alzheimer's disease. FASEB J 18:962–964
Liu CW, Giasson BI, Lewis KA, Lee VM, Demartino GN, Thomas PJ (2005) A precipitating role for truncated alpha-synuclein and the proteasome in alpha-synuclein aggregation: implications for pathogenesis of Parkinson disease. J Biol Chem 280:22670–22678
Lobley A, Whitmore L, Wallace BA (2004) DICHROWEB: an interactive website for the analysis of protein secondary structure from circular dichroism spectra. Bioinformatics 18:211–212
Miyazaki I, Asanuma M (2009) Approaches to prevent dopamine quinone-induced neurotoxicity. Neurochem Res 34:698–706
Norris EH, Giasson BI, Hodara R, Xu S, Trojanowski JQ, Ischiropoulos H, Lee VM (2005) Reversible inhibition of alpha-synuclein fibrillization by dopaminochrome-mediated conformational alterations. J Biol Chem 280:21212–21219
Pham CLL, Leong SL, Ali FE, Kenche VB, Hill AF, Gras SL, Barnham KJ, Cappai R (2009) Dopamine and the dopamine oxidation product 5, 6-dihydroxylindole promote distinct on and off-pathway aggregation of α-synuclein in a pH dependent manner. J Mol Biol 387:771–785
Plaxco KW, Dobson CM (1996) Time-resolved biophysical methods in the study of protein folding. Curr Opin Struct Biol 6:630–636
Polymeropoulos MH, Lavedan C, Leroy E, Ide SE, Dehejia A, Dutra A, Pike B, Root H, Rubenstein J, Boyer R, Stenroos ES, Chandrasekharappa S, Athanassiadou A, Papapetropoulos T, Johnson WG, Lazzarini AM, Duvoisin RC, Di Iorio G, Golbe LI, Nussbaum RL (1997) Mutation in the α-synuclein gene identified in families with Parkinson's disease. Science 276:2045–2047
Qin Z, Hu D, Han S, Hong DP, Fink AL (2007) Role of different regions of alpha-synuclein in the assembly of fibrils. Biochemistry 46:13322–13330
Schuck P (2000) Size distribution analysis of macromolecules by sedimentation velocity ultracentrifugation and Lamm equation modeling. Biophys J 78:1606–1619
Svergun DI (1997) Restoring three-dimensional structure of biopolymers from solution scattering. J Appl Cryst 30:792–797
Svergun DI, Koch MH (2002) Advances in structure analysis using small-angle scattering in solution. Curr Opin Struct Biol 12:654–660
Tashiro M, Kojima M, Kihara H, Kasai K, Kamiyoshihara T, Ueda K, Shimotakahara S (2008) Characterisation of fibrillation process of alpha-synuclein at the initial stage. Biochem Biophys Res Comm 369:910–914
Uversky VN, Li J, Fink AL (2001) Evidence for a partially folded intermediate in α-synuclein fibril formation. J Biol Chem 276:10737–10744
Volkov VV, Svergun DI (2003) Uniqueness of ab initio shape determination in small angle scattering. J Appl Cryst 36:860–864
Whitmore L, Wallace BA (2004) DICHROWEB, an online server for protein secondary structure analyses from circular dichroism spectroscopic data. Nucleic Acids Res 32:W668–W673
Whitmore L, Wallace BA (2008) Protein secondary structure analyses from circular dichroism spectroscopy: methods and reference databases. Biopolymers 89:392–400